Indian Journal of Geo-Marine Science
Vol. 45(10), October 2016, pp. 1264-1271

Relation between Sonic Layer and Mixed layer depth in the Arabian Sea

TVS Udaya Bhaskar[1*] Debadatta Swain[2]
[1]Indian National Centre for Ocean Information Services (INCOIS), Ministry of Earth Science, Pragathinagar (BO), Nizampet (SO), Hyderabad - 500 090, India
[2]School of Earth, Ocean & Climate Sciences, Indian Institute of Technology, Bhubaneswar - 751007, India
*[E.Mail: uday@incois.gov.in]

Received: 13 March 2015; revised 05 January 2016

Seasonal evolution of the sonic layer depth and its relation to mixed layer depth in the Arabian Sea is studied. Monthly sonic layer depth climatology is constructed using Argo temperature and salinity and compared with mixed layer depth. Sonic layer depth showed semiannual variability with peaks during June – August and December – February and lows during pre and post monsoon season. Sonic layer depth is observed to be shallower than mixed layer depth over most of the Arabian Sea except in the southeastern Arabian Sea during winter owing to temperature inversions. Sonic layer and mixed layer depth is observed to have high correlation (> 0.85) over most of the Arabian Sea indicating a good relationship between them, except in south eastern Arabian Sea. SLD is found to be deeper than MLD only in the southeastern AS (SEAS) during the winter season due to the presence of temperature inversions (TI) which are common phenomenon during that period. Advection of cooler low-salinity water over warmer salty SEAS water leads to the formation of TI in SEAS. Sound velocity being sensitive to temperature, results in deepening of SLD in this region. This can be used to understand relation between them to a great degree of accuracy and estimate one from the other.

[Keywords: Sonic Layer Depth, Mixed Layer Depth, Argo, Arabian Sea, Temperature Inversion.**]**

Introduction

Ocean being almost opaque to electromagnetic radiation, sound is the only means to probe the ocean's interior. Ocean acoustic tomography is a tool for synoptic monitoring of large-scale oceanographic features[1]. Conditions of the upper ocean often result in forming a near surface acoustic duct that limits the downward transmission of sound and results in acoustic spreading to be approximately cylindrical[2,3]. Sound trapped in a surface duct is primarily transmitted outward from the source in an expanding disk.

Sonic layer depth (SLD) is the depth of maximum sound speed above the deep sound channel axis or the depth up to which the increasing sound speed penetrates[3,4,5]. SLD has significant strategic implications as it characterizes surface acoustic ducts. Helber et al.,[3] described that there exists a minimum cutoff frequency above which sound tends to be "trapped" near the surface, depending on the SLD. A submerged object goes undetected by surface sonar at a depth of SLD and beyond. Thus, SLD plays an important role in refraction of sound rays travelling in the ocean, which in turn affects the sonar detection ranges. SLD in the ocean is conventionally estimated from sound velocity profile (SVP) which is obtained either by a velocimeter that measures sound speed directly or by using the *in situ* T/S profiles[4,6,7]. The oceanic T/S profiles are affected by many surface and subsurface parameters, which in turn affect acoustic propagation in the ocean. A parameter which has high relation to SLD in the ocean is the mixed layer depth (MLD). MLD is region of ocean with in which the salinity, temperature and density are almost vertically uniform. Also MLD identifies the depth up to which the turbulence near the ocean surface penetrates. For a typical water column, where isothermal and isohaline surface layer depths are equal, MLD and SLD coincides with each other. However, there can be conditions where SLD may be lower or higher than MLD[3]. Since MLD is a commonly known and studied parameter, MLD is often used as a proxy for SLD in scientific and operational applications[3].

In the present study, we examine the relationship and highlight how, when, and where differences between SLD and MLD may occur over the Arabian Sea (AS) on the seasonal cycle. The AS

has a unique geographical location limited in the north by the Asian sub-continent. Consequently, the AS is forced by intense, annually reversing monsoon winds which force the ocean locally, and also excite propagating signals that travel large distances and affect the ocean remotely. During winter monsoon, weak winds bring cool and dry continental air whereas the summer monsoon brings humid maritime air into the AS[8]. Surface circulation of AS also undergoes changes with the changing monsoon system. These semi-annual atmospheric forcings would modulate the thickness of the upper ocean by altering the thermal and mechanical inertia of the layer[9]. During the winter monsoon period, the southeastern AS (SEAS) is influenced by the inflow of low saline waters from the Bay of Bengal (BoB)[10,11]. The combined effect of north equatorial current and southward flowing East Indian Coastal Current (EICC) brings low salinity waters into the AS. As a result, the SEAS is characterized by fresher surface water residing above warmer saltier deep water. SLD and its relation to MLD is impacted by this unique hydrographic structure, making this a interesting region for studying SLD and its relation to MLD. Helber et al.,[3] have done a similar work for Aegean, Marmara, Black and Azov Seas but using available climatological data. However, in the present study we have used Argo datasets to study the SLD and MLD relations in one of the very important regions of the Indian Ocean, the AS. Hence this work can be considered as a application of study by Helber et al.,[3] to the AS in the sense that similar analysis has been employed.

Materials and Methods

Spatio-temporal variability of SLD and the factors responsible for the variability are studied using T/S data from Argo floats. The T/S profiles spanning the years 2002 – 2011 were obtained from "Argo data and products for Indian Ocean" DVD product, released by the Indian National Centre for Ocean Information Services (INCOIS). Details about the DVD product can be obtained from Geetha et al.,[12]. These data sets are made available by United States Global Ocean Data Assimilation Experiment (USGODAE) and Institut français de recherche pour l'exploitation de la mer (IFREMER). International Argo project was envisaged towards building an archival of real-time in situ ocean T/S observations. These profiling floats provide T/S from surface to about 2000 m depth every 5/10 days[13,14]. Figure 1 shows the locations at which about 34354 T/S profiles have been collected through the Argo programme from January 2002 – December 2011 in the study area. The data were made available after subjecting to real time quality control checks as proposed by Wong et al.,[15]. Further these profiles are re-evaluated for their quality via a three-way-quality control system, details of which are given by Udaya Bhaskar et al.,[16].

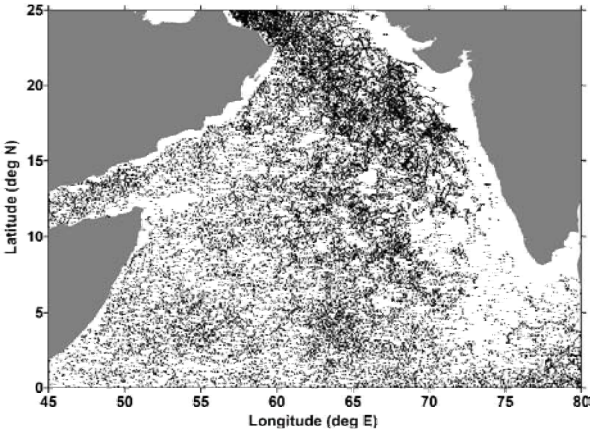

Fig. 1—Location of temperature and salinity profiles obtained from Argo profiling floats used in the study.

Since T/S profile data is unavailable at regular depths for all the floats, we uniformly interpolated the profiles using Akima spline[17] to 1 m depth resolution until 1000 m for all the observations. These interpolated T/S data sets were then used to compute sound velocity at each depth following Fofonoff and Millard[18]. SLD was then estimated from these SVPs based on Helber et al.,[3]. Correspondingly, MLD is estimated from the T/S profiles based on Kara et al.,[19]. Monthly mean SLD and MLD was prepared on 1º X 1º grid using the Kriging method. Kriging is based on the statistical principles and on the assumption that the parameter being interpolated can be treated as a regionalized variable. The advantage of Kriging is that it is an exact interpolator, and the estimation error is provided in the form of the Kriging standard deviation (SD: an analogy to the statistical SD). This method assumes that local means are not necessarily related to the population mean, and therefore uses only the sample in the local neighbourhood of the estimation location. It builds a weighted average of those neighbouring data so as to minimize the estimation variance which can be expressed in terms of the model covariances of the data[20].

Results and Discussion

Monthly Sonic Layer Depth Climatology

The spatial distribution of SLD during January showed deep SLD in excess of 60 m north of 10° N encompassing northwestern AS including the western, central AS and the northeastern region (Figure 2a).

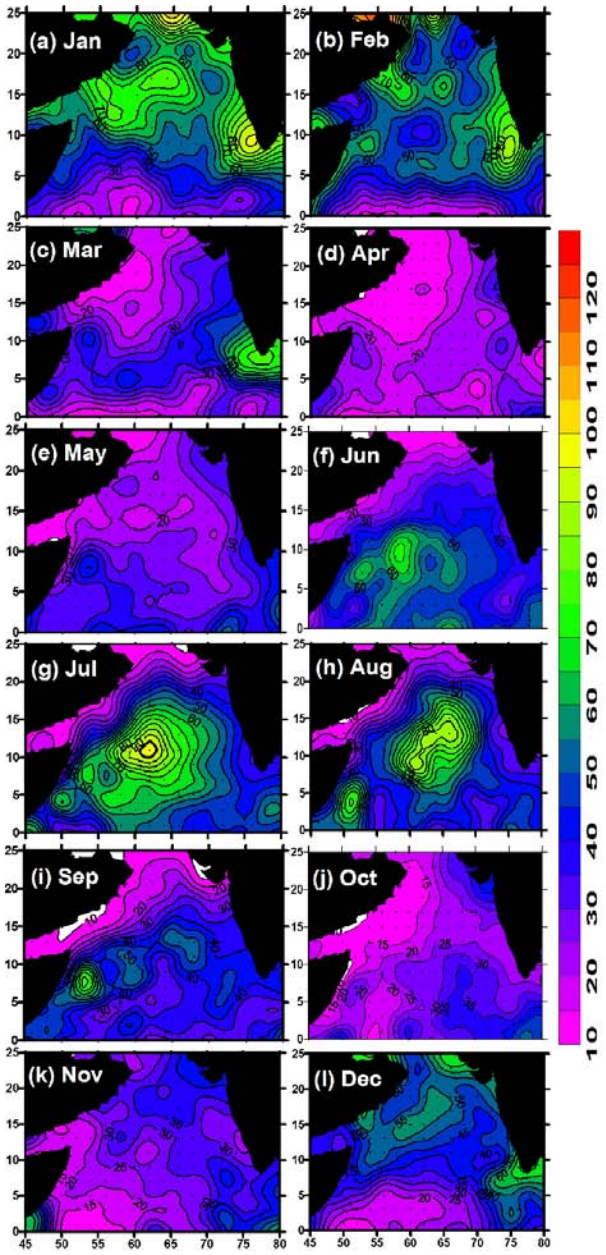

Fig. 2—Monthly mean distribution of SLD (m) in the Arabian Sea during January to December.

These deeper SLD are found to concentrate between 72 - 77° E and 5 - 12° N. The deepest SLD observed in this region was 90 m. South of 5° N the SLD was found to decrease to 15 m. Thus, the spatial variation of SLD in the basin was about 90 m. During February, SLD varied almost similar to that of January. The region of deepest SLD moved northwestern and located between 50 and 60° E. The region of shallower SLD was seen in the equatorial AS as appeared in the previous month, and the shallower SLD orienting zonally along the equator between 0° and 5° N (Figure 2b). The deeper SLD found in the SEAS during January is found to persist in this month also. During March, most part of the AS showed shallow SLD less than 30 m, except at two locations, one around SEAS and the other in the northwestern (Persian Gulf) region (Figure 2c). The shallowest SLD (~ 15 m) occurred parallel along the coast of Arabia and also southern parts close to equator. In April, SLD in most part of the AS was shallower than 20 m (Figure 2d). The deep SLD found in the SEAS during the previous month vanished. North of 10° N, shoaling intensified with SLD reaching 15 m.

During the month of May, SLD remained same as that observed in April with SLD shallower than 20 m (Figure 2e). However, relatively deeper SLD of 30 m was observed south of 10° N, and along the west coast of Indian peninsula. In June, the region of deep SLD was observed south of 12° N and west of 70° E (Figure 2f). Most parts of AS south of 12° N has deep SLD (> 50 m) with the deepest value of 70 m in the southwestern AS. Along the boundary of the Indian peninsula, SLD was shallow (~30-40 m). SLD decreased rapidly north of 12° N and the shallowest SLD of 10 m was concentrated close to the Gulf of Oman. Similarly, near the Gulf of Aden, SLD decreased rapidly from 40 m to 20 m. The spatial distribution of SLD during July showed marked difference in comparison to June, with SLD deeper than 80 m observed in the central AS (Figure 2g). The deepest SLD of 100 m was centered between 60 - 65° E and 8 - 12° N during this period. Shallowest SLD (20 – 40 m) is found orienting parallel to coast of Oman and western Indian peninsula. North of 20° N, shallowest SLD values of 10 m were observed close to Gulf of Oman as that found in the month of June. In August also, the spatial distribution of SLD was similar to that of July, except that shallower SLD was noticed south of 5° N and east of 53° E (Figure 2h). However, the deepest SLD shoaled to 85 m from 100 m as observed in July. The rapid shoaling of SLD seen all along the coast of Oman and Indian peninsula in July intensified further with the shallowest SLD recording of 10 m.

During September, the region of deep SLD in the central AS as observed in the month of August disappeared (Figure 2i) with a patch of high SLD found near the Somalia Coast. The region of

shallow SLD (30 – 40 m) further expanded from the Gulf of Oman towards south reaching up to 12° N. Shallow SLD (~ 30 m) was observed south of 5° N. The shallow SLD observed all along the Oman coast and the Indian peninsula remained similar to that observed in August. The deepest SLD of 60 m was found along the Somalia coast. In October the area of shallow SLD expanded to the whole of AS and SLD is found to vary between 15 – 35 m (Figure 2j). SLD values of 15 m, was found to run parallel from Gulf of Aden along the Oman coast up to the Gulf of Oman. Deepest SLD of 50 m was recorded in eastern equatorial region south of the Indian tip. The basin-wide SLD in November was shallower than 35 m except in two smaller regions – one in the southwestern region (Somali coast) and the other near eastern equatorial region between 75 - 80° E (Figure 2k). The deepest SLD was 55 m in November. In December, the spatial pattern of SLD changed in comparison to November, with deep SLD values of 50 m found all along north of 10° N. Deeper SLD of greater than 70 m was observed along the northeastern AS, which was attached to the deep SLD of 55 m in the central AS (Figure 2l). Deeper SLD values of 60 m were also observed along the SEAS.

Factors responsible for deep SLD in SEAS

Seasonal variation of MLD in the AS is studies in detail using Argo data by Udaya Bhaskar et al., [21]. During winter monsoon season (December to February), deep SLDs are observed in the AS. This is consequence of the convective process resulting in mixing and deepening the sonic layer as is the case with the MLD[21]. In addition to this, anomalously deep SLD in contrast to shallow MLD is observed in the SEAS which need to be investigated. This deep SLD can be explained in context of ocean-atmosphere conditions. Temperature Inversions (TI, where the vertical gradient in temperature increases with the depth in contrast to the normal decrease) are a stable winter time (December – February) feature of the SEAS[22,23,24]. In the SEAS, TI starts appearing during early December and disappears by early March and occurs as deep as 80 m during January[23,24]. Figure 3 presents zonal and meridional sections of T/S in SEAS for the month of January. In SEAS, the upper layer stratification is dominated by salinity effects during December – February. During this period the East Indian Coastal Current and Winter Monsoon Current act together to bring low-salinity water from the BoB into the SEAS, which is cooler than ambient waters. The advection of cooler water over the warmer water directly leads to the formation of TI (Figure 3b).

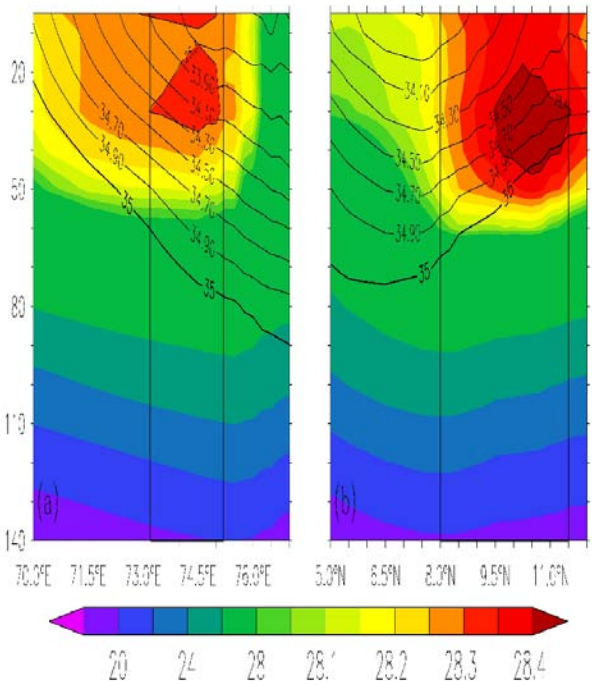

Fig. 3—Temperature in the SEAS during January (a) averaged along 5-12° N (b) averaged along 70 – 77° E. Overlaid contour lines indicate salinity (range 33.5 – 35 PSU). Contour interval for temperature is 2° C from 18 – 28 and 0.05° C from 28 – 28.4° C, and 0.2 PSU for salinity.

Moreover SEAS is also a region of net heat gain (Thadathil and Gosh[22]) from atmosphere during December – February due to very low (< 4 m/s) winds. Since sound velocity is more sensitive to temperature, it increases starting from surface up to the depth of inversion which in turn resulted in deepening of SLD in SEAS. Hence the deep SLD in the SEAS is a consequence of prevailing atmospheric conditions (net heat gain), and advection of cooler low saline waters from BoB which resulted in formation TI, which in turn resulted in increase in sound velocity up to the depth of TI. Similar cases of deep SLDs in comparison to MLDs are observed by Helber et al., (2009) in Black Sea, a region which is heavily influenced by river inputs along with precipitation exceeding evaporation losses. As a result of this, the Black Sea is characterized by fresher surface water residing over warmer saltier deep waters (similar to SEAS). Consequently deeper SLDs in comparison to MLD were observed during winter (January, February and part of March) in southwestern Black Sea and in Aegean Sea, which support our observations in SEAS.

Table 1—Basin averaged difference of SLD and MLD (SLD – MLD). Standard deviations are calculated from the entire domain (45° to 80° E, 0 to 25° N).

Parameter (m)	Jan	Feb	Mar	Apr	May	Jun	Jul	Aug	Sep	Oct	Nov	Dec
SLD–MLD	-1	-1	-6	-8	-7	-5	-5	-3	-7	-8	-6	-4
Stdev	11	14	11	5	3	3	5	10	7	6	5	9

Differences between MLD and SLD

Information regarding the upper ocean structure can be obtained by comparing surface layer phenomenon like SLD and MLD. When the SLD is deeper than MLD, T/S both tend to increase with depth there by sustaining the TIs formed (typical case of SEAS profiles). Salinity must increase continuously with depth, else the profile would be unstable. On the other hand, when the MLD is deeper than the SLD, it is owing to the response of SLD to small sound speed maxima (local maxima) in profiles that are comparatively uniform with depth. To explore these relationships further, a thorough analysis is undertaken to check whether SLD is typically deeper than, shallower than, or identical to MLD in the study region.

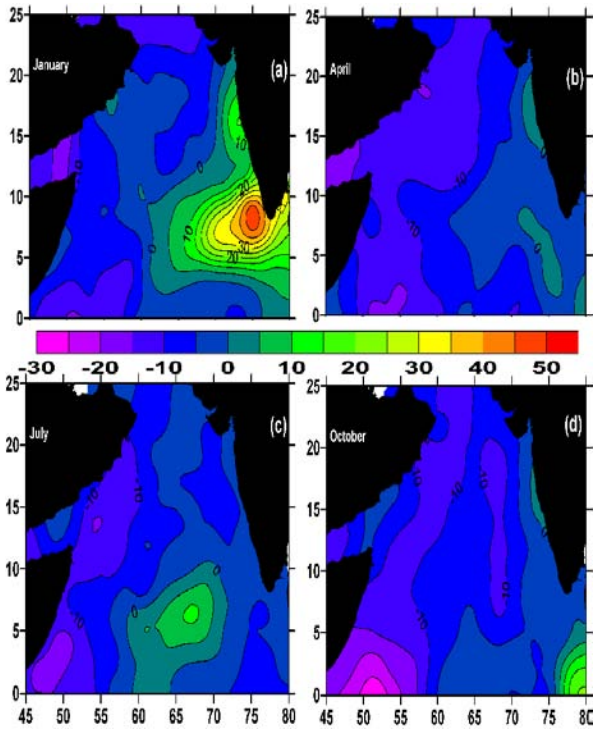

Fig. 4—Differences between SLD and MLD for: (a) January, (b) April, (c) July, (d) October representative of winter monsoon, pre monsoon, summer monsoon, post monsoon seasons respectively.

Differences between monthly mean SLD and MLD are computed and shown in Figure 4. It is clearly observed from Figure that, SLD can be deeper or shallower than MLD depending on the region and season. Two distinct features are observed in the differences between SLD and MLD. The SLD is typically much deeper than MLD in the SEAS during December – March (Winter monsoon period). When SLD deepened to 80 m, MLD remained shallow (~ 30 m). However, the spread of deep SLD is restricted to SEAS and its dominance is not observed in the basin-wide average (Table 1). The variance of the basin-wide difference fields is larger during winter and early summer due to the deep SLD observed in comparison to MLD in the AS. The main feature observed in the AS is that the MLD is deeper than SLD over most of the AS (negative values over most of AS) throughout the year, but the magnitude of this bias is generally smaller. The values for the difference SLD – MLD shown in Table 1 are negative for all months with the least recording during the months January - February. The least values recorded during the winter period can be attributed to the presence of deep SLD in the SEAS which influenced the basin wide average.

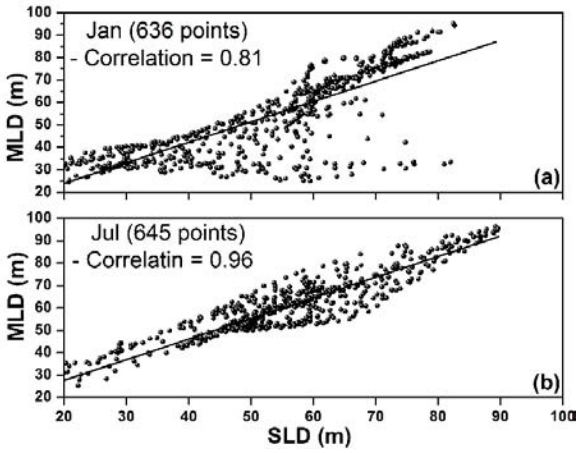

Fig. 5—Scatters between SLD and MLD gridded fields for (a) January (R = 0.81), and (b) July (R = 0.96).

To further illustrate the differences between SLD and MLD a scatter diagram was produced for January and July months representing the winter and summer monsoon periods respectively where the SLD is observed to be peaking on the annual cycle. The Kriging interpolation field data is used in generating the figures. For January, there exists a statistically significant linear correlation coefficient of 0.81.There is one lobe on the lower right side of Figure 5a where MLD is found to vary between 20 and 30 m and SLD is between 60 and 80 m that represents values in the SEAS. This lobes reveals the role played by salinity in deepening SLD in comparison to MLD. For July, the statistically significant linear correlation coefficient is 0.96 (Figure 5b) which clearly reveals the extent of mixing that takes place due to the high winds prevalent during summer monsoon season. Since, the surface layers are thoroughly mixed making the properties of salinity and temperature more uniform in the near surface, there is little variation between MLD and SLD. During the summer monsoon, the distribution of SLD resembles that of MLD spatially in almost all details resulting in high correlation coefficient.

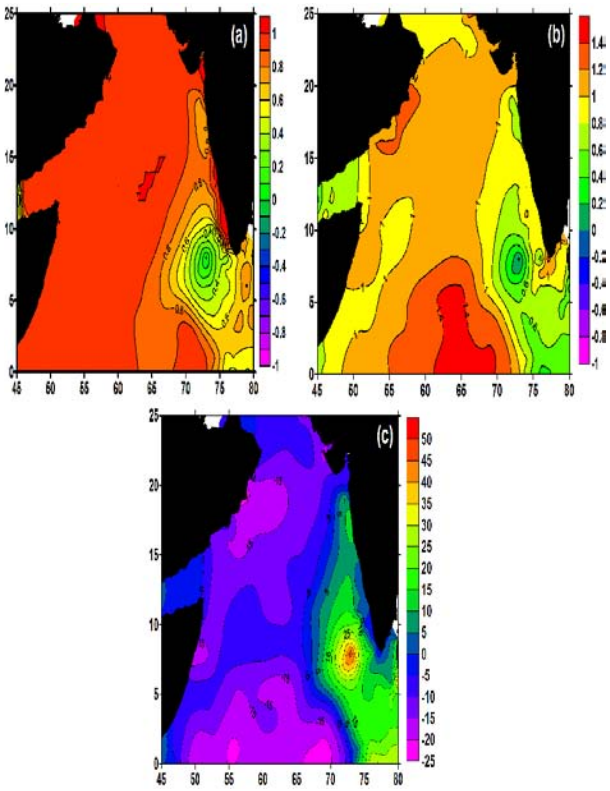

Fig. 6—Spatial variation of (a) correlation coefficient (b) slope of least square line (c) intercept of least square line between SLD and MLD obtained using the gridded data over the seasonal cycle.

Relationship between SLD and MLD

Following Helber et al.,[3] we sought a simple relationship between SLD and MLD values over the seasonal cycle in AS. This could help identify regions where MLD can be used as proxy for SLD when the required sound profiles data are not available. For this, the time series of SLD and MLD over the seasonal cycle is used. The statistical relationships between MLD (X) and SLD (Y) based on the 12 monthly mean values at each grid point are expressed as follows:

$$R = \frac{1}{n}\sum_{i=1}^{n}(X_i - \overline{X})(Y_i - \overline{Y})/(\sigma_X \sigma_Y) \qquad (1)$$

Where

$$Y = a + bX + c \qquad (2)$$

and n = 12, R is the correlation coefficient, and $\overline{X}$ ($\overline{Y}$) and σ_X (σ_Y) are the mean and standard deviations of MLD (SLD) values, respectively. In the regression Eq. (2), Y is the dependent variable, X is the independent variable (or covariate), a is the intercept, b is the slope or regression coefficient, and c is the error term. The regression equation will specify the average magnitude of the expected change in SLD for the given MLD climatology at each grid point. First correlation between SLD and MLD over the seasonal cycle is determined. The strength of the linear relationship between SLD and MLD is determined by the R values (Eq. (1)). The resulting correlations given in Figure 6a clearly reveals strong and positive values (> 0.8) over most of the domain except in the SEAS.

Given the significant correlation values over almost the AS, a linear regression can be used to examine the relationship between SLD and MLD except for the SEAS. The regression relation is found with an objective to fit a straight line to values between SLD and MLD obtained at each grid over the seasonal cycle. The process is done at each grid point based on monthly mean SLD and MLD time series. Slope and intercept values of the least square line are then computed as described in Eq. (2). Figure 6b shows the slope of the fitted regression between SLD and MLD. In particular, slope values ranging between 1 and 1.2 are observed in most of the AS. For the SEAS the slope values are observed to range between 0 and 0.6 (Figure 6b), while the intercept is positive

(Figure 6c) indicating that SLD is deeper than MLD in this part of AS. This simple relation can be used to understand MLD and SLD relation in the Arabian Sea with a great degree of accuracy.

Conclusions

Deep SLD is observed to occurs in the SEAS during winter months of December – February (Winter monsoon period). The deepening starts early December and observed to disappear by March. Rest of the AS is observed to have SLD similar to that of MLD. This deep SLD in SEAS is due to the inflow of low saline waters from BoB by a combination of southward flowing east India Coastal current and winter monsoon currents. The advection of cold less saline waters over warmer high saline water cause the formation of TIs, which in turn cause the SLD to deepen as sound velocity is more sensitive to temperature than salinity. However, MLD remains shallower owing to high stratification caused by the low saline water in the SEAS. Simple statistical relationship between SLD and MLD values over the seasonal cycle in AS is determined. The correlation clearly revealed strong and positive values (> 0.8) over most of the domain except in the SEAS which is the result of deeper/shallower SLD/MLD particularly during winter. A linear statistical relationship is established based on statistically significant correlation values between SLD and MLD which can be used to estimate one from the other when needed.

Acknowledgements

Authors thank Director, INCOIS for encouragement and for proving the necessary infrastructure to carry out this work. Argo data is made available freely by the International Argo Community. This is INCOIS contribution number 237.

References

1. Munk, W., and Wunsch, C., Ocean acoustic tomography: a scheme for large scale monitoring, *Deep-Sea Res.*, 26A(1979) 123 – 161.
2. Urick, R. J., *Principles of Underwater Sound*, (McGraw-Hill, New York) 1983, pp. 423.
3. Helber, R. W., Kara, A. B., Barron, C. N., and T. P. Boyer., Mixed layer depth in the Aegean, Marmara, Black and Azov Seas: Part II: Relation to the sonic layer depth, *J. Mar. Syst.,* Doi: 10.1016/j.jmarsys.2009.01.023 (2009) 181 - 190.
4. Udaya Bhaskar, T.V.S., Swain, D., and Ravichandran, M., Seasonal variability of Sonic Layer depth in the central Arabian Sea, *Ocean. Sci. J.*, 43 (2008) 147 – 152.
5. Etter, C. P., *Underwater Acoustic Modelling: Principles, Techniques and Applications*. 2nd ed., (E & FN Spon, London) 1996, pp. 344.
6. Jain, S., Ali, M.M., and Sen. P.N., Estimation of sonic layer depth from surface parameters. *Geophys. Res. Lett*., 34 L17602.doi:10.1029/2007GL030577 (2007).
7. Lü, L.G., Chen, H.X., and Yuan, Y.L., Spatial and temporal variations of sound speed at the PN Section, *J. Oceanogr*., 60(2003) 673-679.
8. Weller, R. A., Fischer, A. S., Rudnick, D. L., Eriksen, C. C., Dickey, T. D., Marra, J., Fox, C., and Leben, R., Moored observations of upper-ocean response to the monsoons in the Arabian Sea during 1994-1995, *Deep-Sea. Res. PT. II.*, 49 (2002) 2195 – 2230.
9. Prasanna Kumar, S., and Narveker, J., Seasonal variability of mixed layer in the central Arabian Sea and its implication to nutrients and primary productivity, *Deep-Sea. Res. II.*, 52 (2005) 1848 - 1861.
10. Schott, F., Reppin, J., and Fischer, J., Currents and transports of the Monsoon Current south of Sri Lanka. *J. Geophys. Res.,* 99 (1994) 25127-25141.
11. Prasanna Kumar, S., Narvekar, J., Kumar, A., Shaji, C., Anand, P., Sabu, P., Rijomon, G., Josia, J., Jayaraj, K. A., Radhika, A., and Nair, K. K. C., Intrusion of the Bay of Bengal water into the Arabian Sea during winter monsoon and associated chemical and bioligical response, *Geophys. Res. Lett*., 31 (2004) L15304, doi:1029/2004GL020247.
12. Geetha, G., Udaya Bhaskar, T.V.S., Pattabhi Rama Rao. E., Argo data and products of Indian Ocean for low bandwidth users. *Int. J. Ocean Oceanogr*., 5 (2011) 1 – 8.
13. Argo Science Team., The Global Array of Profiling Floats, in: Observing Oceans in the 21st Century, ed. By C. Z. Koblinsky and N. R. Smith, (Godae Proj. Off., Bur. Meteorol., Melbourne, Australia) 2001, pp. 248 – 258.
14. Ravichandran M., Vinayachandran, P. N., Joseph, S., and Radhakrishnan, K., Results from the first Argo float deployed by India, *Curr. Sci.*, 86 (2004) 651 – 659.
15. Wong, A., R. Keeley, Carval, T., and the Argo Data Management Team., *Argo quality control manual*, *Ver. 3.0*, doi:10.13155/33951 (2015).
16. Udaya Bhaskar, T. V. S., Pattabhi Rama. Rao, E., Venkat Shesu, R., and Devender, R., A note on three way quality control of Argo temperature and salinity profiles - a semi-automated approach at INCOIS, *Int. J. Earth Sci. Eng.*, 5 (2013) 1510 – 1514.
17. Akima, H., A new method of interpolation and smooth curve fitting based on local procedures. *J. Assoc. Comp. Mach*., 17 (1970) 589–602.
18. Fofonoff, N. P., and Millard, R. C., Algorithms for computations of fundamental properties of seawater, *Unesco Technical Papers in Marine Science.*, 44 (1983) pp 53.
19. Kara, A. B., Rochford, P. A., and Hurlburt, H. E., An optimal definition for ocean mixed layer depth. *J. Geophys. Res.,* 105 (2000) 16 803–16 821.
20. Wackernagel, H., *Multivariate Geostatistics*. 2nd ed., (Springer-Verlag, New York) 1998, pp 291.

21. Udaya bhaskar, T.V.S., Swain, D., Ravichandran, M., Inferring mixed layer depth variability in the Arabian Sea from Argo observations, *J. Mar. Res*., 64 (2006) 393 – 406.
22. Thadathil, P., and Gosh, A. K., Surface layer temperature invsersion in the Arabian Sea during winter, *J. Oceanogr*., 48, (1992) 293 – 304.
23. Shankar, D., Goplakrishna, V. V., Shenoi, S. S. C., Durand, F., Shetye, S. R., Rajan, C. K., Johnson, Z., Araligiadad, N., and Michael, G. S., Observational evidence for westward propagation of temperature inversions in the southeastern Arabian Sea, *Geophys. Res. Lett*., 31 (2004) L08305.
24. Kurian, J., and Vinaychandran, P.N., Formation mechanisms of temperature inversions in the southeastern Arabian Sea, *Geophys. Res. Lett*., 33 (2006) L17611.